References

1. Ryan, E.A., Lakey, J.R., Paty, B.W., Imes, S., Korbutt, G.S., Kneteman, N.M., Bigam, D., Rajotte, R.V., and Shapiro, A.M. Successful islet transplantation: continued insulin reserve provides long-term glycemic control. Diabetes **51,** 2148, 2002.
2. Froud, T., Ricordi, C., Baidal, D.A., Hafiz, M.M., Ponte, G., Cure, P., Pileggi, A., Poggioli, R., Ichii, H., Khan, A., Ferreira, J.V., Pugliese, A., Esquenazi, V.V., Kenyon, N.S., and Alejandro, R. Cultured islets and steroid-free immunosuppression: Miami experience. Am J Transplant **5,** 2037, 2005.
3. Bennet, W., Groth, C.G., Larsson, R., Nilsson, B., and Korsgren, O. Isolated human islets trigger an instant blood mediated inflammatory reaction: implications for intraportal islet transplantation as a treatment for patients with type 1 diabetes. Ups J Med Sci **105,** 125, 2000.
4. Rood, P.P.M., Bottino, R., Balamurugan, A.N., Smetanka, C., Ayares, D., Groth, C.G., Murase, N., Cooper, D.K.C., and Trucco, M. Reduction of early graft loss after intraportal porcine islet transplantation in monkeys. Transplantation **83,** 202, 2007.
5. Reece-Smith, H., DuToit, D.F., McShane, P., and Morris, P.J. Prolonged survival of pancreatic islet allografts transplanted beneath the real capsule. Transplantation **31,** 305, 1981.
6. Finch, D.R., Wise, P.H., and Morris, P.J. Successful intrasplenic transplantation of syngeneic and allogenic isolated pancreatic islets. Diabetologia **13,** 195, 1977.
7. Axen, K.V., and Pi-Sunyer, F.X. Long-term reversal of streptozotocin-induced diabetes in rats by intramuscular islet implantation. Transplantation **31,** 439, 1981.
8. Kin, T., Korbutt, G.S., and Rajotte, R.V. Survival and metabolic function of syngeneic rat islet grafts transplanted in the omental pouch. Am J Transplant **3,** 281, 2003.
9. Kemp, C.B., Knight, M.J., Scharp, D.W., Ballinger, W.F., and Lacy, P.E. Effect of transplantation site on the results of pancreatic islet isografts in diabetic rats. Diabetologia **9,** 486, 1973.
10. Kawakami, Y., Iwata, H., Gu, Y.J., Miyamoto, M., Murakami, Y., Balamurugan, A.N., Imamura, M., and Inoue, K. Successful subcutaneous pancreatic islet transplantation using an angiogenic growth factor-releasing device. Pancreas **23,** 375, 2001.
11. Bharat, A., Benshoff, N., Olack, B., Ramachandran, S., Desai, N.M., and Mohanakumar, T. Novel *in vivo* murine model to study islet potency: engraftment and function. Transplantation **79,** 1627, 2005.
12. Pileggi, A., Molano, R.D., Ricordi, C., Zahr, E., Collins, J., Valdes, R., and Inveradi, L. Reversal of diabetes by pancreatic islet transplantation into a subcutaneous, neovascularized device. Transplantation **81,** 1318, 2006.
13. Rafael, E., Wu, G.S., Hultenby, K., Tibell, A., and Wernerson, A. Improved survival of macroencapsulated islets of Langerhans by preimplantation of the immunoisolating device: a morphometric study. Cell Transplant **12,** 407, 2003.
14. Cao, Y., Sun, Z., Liao, L., Meng, Y., Han, Q., and Zhao, R.C. Human adipose tissue-derived stem cells differentiate into endothelial cells *in vitro* and improve postnatal neovascularization *in vivo*. Biochem Biophys Res Commun **332,** 370, 2005.
15. Planat-Benard, V., Silvestre, J.S., Cousin, B., Andre, M., Nibbelink, M., Tamarat, R., Clergue, M., Manneville, C., Saillan-Barreau, C., Duriez, M., Tedgui, A., Levy, B., Penicaud, L., and Casteilla, L. Plasticity of human adipose lineage cells toward endothelial cells. Circulation **109,** 656, 2004.
16. Moon, M.H., Kim, S.Y., Kim, Y.J., Kim, S.J., Lee, J.B., Bae, Y.C., Sung, S.M., and Jung, J.S. Human adipose tissue-derived mesenchymal stem cells improve postnatal neovascularization in a mouse model of hindlimb ischemia. Cell Physiol Biochem **17,** 279, 2006.
17. Sumi, M., Sata, M., Toya, N., Yanaga, K., Ohki, T., and Nagai, R. Transplantation of adipose stromal cells, but not mature adipocytes, augments ischemia-induced angiogenesis. Life Sci **80,** 559, 2007.
18. Matsumoto, D., Sato, K., Gonda, K., Takaki, Y., Shigeura, T., Sato, T., Aiba-Kojima, E., Iizuka, F., Inoue, K., Suga, H., and Yoshioka, K. Cell-assisted lipotransfer: supportive use of human adipose-derived cells for soft tissue augmentation with lipoinjection. Tissue Eng **12,** 3375, 2006.
19. Cinti, S., Cigolini, M., Bosello, O., and Björntorp, P. A morphological study of the adipocyte precursor. Submicrosc Cytol **16,** 243, 1984.
20. Gotoh, M., Maki, T., Kiyoizumi, T., Satomi, S., and Monaco, A.P. An improved method for isolation of mouse pancreatic islets. Transplantation **40,** 437, 1985.
21. Clark, H., Barbari, T.A., Stump, K., and Rao, G. Histologic evaluation of the inflammatory response around implanted hollow fiber membranes. J Biomed Mater Res **52,** 183, 2000.
22. Nakagami, H., Maeda, K., Morishita, R., Iguchi, S., Nishikawa, T., Takami, Y., Kikuchi, Y., Saito, Y., Tamai, K., Ogihara, T., and Kaneda, Y. Novel autologous cell therapy in ischemic limb disease through growth factor secretion by cultured adipose tissue-derived stromal cells. Arterioscler Thromb Vasc Biol **25,** 2542, 2005.
23. Rehman, J., Traktuev, D., Li, J., Merfeld-Clauss, S., Temm-Grove, C.J., Bovenkerk, J.E., Pell, C.L., Johnstone, B.H., Considine, R.V., and March, K.L. Secretion of angiogenic and antiapoptotic factors by human adipose stromal cells. Circulation **109,** 1292, 2004.
24. Chen, X., Zhang, X., Larson, C., Chen, F., Kissler, H., and Kaufman, D.B. The epididymal fat pad as a transplant site for minimal islet mass. Transplantation **84,** 122, 2007.
25. Bonner-Weir, S., and Weir, G.C. New sources of pancreatic beta-cells. Nat Biotechnol **23,** 857, 2005.
26. Okura, H., Matsuyama, A., Komoda, H., Fumimoto, Y., Yanagisawa, T., Nishida, T., Noguchi, S., and Sawa Y. Transdifferentiation of human adipose tissue-derived stromal cells into insulin-producing clusters. Abstract presented at the International Society for Stem Cell Research Meeting, Philadelphia, PA, 2008 (Abstract no. 171).

Address reprint requests to:
Akifumi Matsuyama, M.D., Ph.D.
Medical Center for Translational Research
Osaka University Hospital
2-15 Yamada-oka, Suita
Osaka 565-0871
Japan

E-mail: akifumi-matsuyama@umin.ac.jp

Received: October 7, 2008
Accepted: December 22, 2008
Online Publication Date:

AUTHOR QUERY FOR TEN-2008-0555-FUMIMOTO

AU1: Please mention academic degrees for the author Anna Nagao.
AU2: Disclosure Statement accurate? If not, please amend as needed.
AU3: "*$p < 0.05$; **$p < 0.01$" given in the legend, but "* < 0.005; ** < 0.001" given in Fig. 3. Please check.

Radiotherapy and Oncology 92 (2009) 89–95

Contents lists available at ScienceDirect

Radiotherapy and Oncology

journal homepage: www.thegreenjournal.com

Boron neutron capture therapy

Impact of accelerator-based boron neutron capture therapy (AB-BNCT) on the treatment of multiple liver tumors and malignant pleural mesothelioma

Minoru Suzuki [a,*], Hiroki Tanaka [b], Yoshinori Sakurai [b], Genro Kashino [a], Liu Yong [a], Shinichiro Masunaga [a], Yuko Kinashi [a], Toshinori Mitsumoto [c], Satoru Yajima [c], Hiroshi Tsutsui [c], Takemi Sato [c], Akira Maruhashi [b], Koji Ono [a]

[a] Particle Radiation Oncology Research Center, Research Reactor Institute, Kyoto University, Osaka, Japan
[b] Radiation Medical Physics Laboratory, Research Reactor Institute, Kyoto University, Osaka, Japan
[c] Sumitomo Heavy Industries, Ltd., Tokyo, Japan

ARTICLE INFO

Article history:
Received 14 October 2008
Received in revised form 9 January 2009
Accepted 11 January 2009
Available online 28 March 2009

Keywords:
Accelerator-based neutron source
Boron neutron capture therapy
Liver tumor
Malignant pleural mesothelioma

ABSTRACT

Background and purpose: To confirm the feasibility of accelerator-based BNCT (AB-BNCT) for treatment of multiple liver tumors and malignant pleural mesothelioma (MPM), we compared dose distribution and irradiation time between AB-BNCT and reactor-based BNCT (RB-BNCT).
Material and methods: We constructed treatment plans for AB-BNCT and RB-BNCT of four multiple liver tumors and six MPM. The neutron beam data on RB-BNCT were those from the research reactor at Kyoto University Research Reactor Institute (KURRI). The irradiation time and dose–volume histogram data were assessed for each BNCT system.
Results: In BNCT for multiple liver tumors, when the 5 Gy-Eq dose was delivered as the mean dose to the healthy liver tissues, the mean dose delivered to the liver tumors by AB-BNCT and RB-BNCT was 68.1 and 65.1 Gy-Eq, respectively. In BNCT for MPM, when the mean lung dose to the normal ipsilateral lung was 5 Gy-Eq, the mean dose delivered to the MPM tumor by AB-BNCT and RB-BNCT was 20.2 and 19.9 Gy-Eq, respectively. Dose distribution analysis revealed that AB-BNCT is superior to RB-BNCT for treatment of deep-seated tumors.
Conclusions: The feasibility of the AB-BNCT system constructed at our institute was confirmed from a clinical viewpoint in BNCT for multiple liver tumors and MPM.
 Radiotherapy and Oncology 92 (2009) 89–95

Boron neutron capture therapy (BNCT) is based on a nuclear reaction: non-radioactive isotope ^{10}B atoms that have absorbed low energy (<0.5 eV) neutrons disintegrate into alpha (^{4}He) particles and recoiled lithium nuclei (^{7}Li). These particles deposit large energy along their very short paths (<10 μm), whose lengths are equal to or shorter than a typical cell size [1,2]. Malignant cells with ^{10}B are thus destroyed following thermal neutron irradiation by these high linear energy (LET) particles. If a sufficient number of ^{10}B atoms accumulate in the tumor cells and the gradient of the ^{10}B concentrations between the tumor and the surrounding normal tissues is large, then boron neutron capture irradiation will be selectively delivered to the tumor.

Selective high LET particle irradiation to cancer cells is a unique property of BNCT, which is an advantage over other radiotherapy modalities. For the use of this unique property, we have continued preclinical studies on application of BNCT to tumors located in radiosensitive organs, such as liver and lung [3,4]. In our previous studies, the feasibility of BNCT for treating multiple liver tumors and inoperable malignant pleural mesothelioma (MPM) was confirmed from the viewpoint of dose distribution [5,6]. Based on these preclinical studies, we have carried out clinical BNCT for multiple liver tumors and MPM since 2005 at Kyoto University Research Reactor Institute (KURRI). One patient with asbestos-induced MPM and three cases of multiple liver tumors have already been treated with BNCT [7,8].

To deal with the increasing number of candidates for BNCT, development of an accelerator-based BNCT (AB-BNCT) system is a prerequisite. Construction of an AB-BNCT system at KURRI was started in June 2008 and was finished in December 2008. To prepare the protocol for clinical studies using the AB-BNCT system, comparison of the parameters for dose distribution and irradiation time between Kyoto University reactor (KUR)-based BNCT (RB-BNCT) and the AB-BNCT is needed. The aim of the present study was to investigate the advantages of AB-BNCT over RB-BNCT for multiple liver tumors and MPM.

* Corresponding author. Address: Particle Radiation Oncology Research Center, Research Reactor Institute, Kyoto University, 2-1010, Asashiro-nishi, Kumatori-cho, Sennan-gun, Osaka 590-0494, Japan.
E-mail address: msuzuki@rri.kyoto-u.ac.jp (M. Suzuki).

0167-8140/$ - see front matter © 2009 Elsevier Ireland Ltd. All rights reserved.
doi:10.1016/j.radonc.2009.01.010

Material and methods

Accelerator

Our AB-BNCT system consists of a cyclotron accelerator that produces a proton beam of ~2 mA at 30 MeV, beam transport system, beam scanning system on the beryllium target, target cooling system, neutron-beam-shaping assembly (BSA), multileaf collimator, and an irradiation bed for patients in both sitting and decubitus positions. Fig. 1 shows a schematic layout of the BSA for production of epi-thermal neutrons.

The Li(p,n) reaction at low proton energy is widely accepted as the most promising for epi-thermal neutron generation [9]. However, we selected the Be(p,n) reaction with 30 MeV for our AB-BNCT system because: (1) the system using Li(p,n) reaction needs an accelerator with a current of >5 mA to yield an intensity of epi-thermal neutron flux of 1×10^9 n/cm^2/s. No accelerator is presently available to achieve such a high current; (2) it is difficult to stably operate a lithium target with heat >10 kW because the 180 °C melting point of lithium is much lower than that of beryllium, which is 1278 °C; and (3) the Be(p,n) reaction with 30 MeV has a higher neutron yield compared with the Li(p,n) reaction. The neutron yield of the Li(p,n) reaction with 1.9 MeV (near threshold) is about 2.4×10^{-6} (neutrons/proton) [9]. Whereas, the neutron yield of the Be(p,n) reaction with 30 MeV is about 3.0×10^{-2} (neutrons/proton) [10].

The reaction of a proton with the beryllium target emits high energy neutrons at up to 28 MeV in the 0° direction. The 0° neutron yield is the largest. The BSA consists of lead, iron, calcium fluoride, and aluminum for reducing neutron energy and shaping an epi-thermal neutron beam. The BSA is surrounded by polyethylene material for shielding fast neutrons and for decreasing radiation to the patient's body. The γ-ray dose contamination in the treatment neutron beam increases because of γ-rays coming from the neutron capture in hydrogen materials such as polyethylene. However, the γ-ray dose contamination per epi-thermal neutron in a treatment beam under free-air conditions is 7.75×10^{-14} Gy cm^2 (epi-thermal region is from 0.5 eV to 40 keV). This value is sufficiently below than the IAEA-TECDOC-1223 target value of 2×10^{-13} [11].

KUR

KUR is a light water-moderated, tank-type nuclear research reactor, with a nominal power of 5 MW. The Heavy Water Neutron Irradiation Facility (HWNIF) is a bio-medical facility at KURRI. The facility has been previously described in detail [12,13]. The higher energy neutrons are moderated by the epi-thermal neutron moderator, which is the mixture of aluminum and heavy water (80%/20% in volume). The heavy-water spectrum shifter is installed outside of the epi-thermal neutron moderator, for control of the neutron-energy spectrum. The total heavy-water thickness can be changed from 0 to 90 cm in 10-cm increments. The thermal neutron filters of cadmium and boral are installed outside of the spectrum shifter, to regulate the thermal neutron component. The apertures of these filters are changed from 0 to 62 cm. Outside of the filters, the bismuth layer is placed for γ-ray elimination. In this facility, neutron beams with various energy spectra from almost pure thermal to epi-thermal are available by controlling the heavy-water thickness in the spectrum shifter, and by the opening and closing of the cadmium and boral thermal neutron filters.

Comparison of neutron spectra

A comparison has been carried out between the neutron spectra at the output port in air for AB-BNCT and RB-BNCT. For the KUR, the neutron spectrum was measured by activation of gold foils. For the accelerator-based neutron source, the neutron spectrum was obtained by simulations from a calculated neutron source.

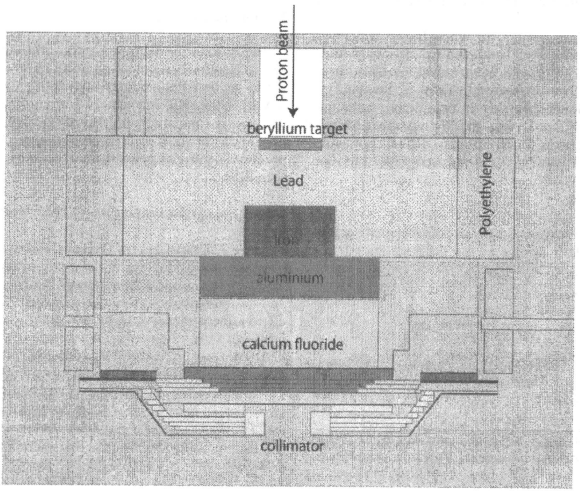

Fig. 1. Schematic layout of BSA for production of epi-thermal neutrons based on beryllium (p,n) reaction using 30 MeV proton beam.

Assumption and parameters for BNCT treatment planning

The conditions and parameters in BNCT treatment planning are summarized in Table 1. The parameters were approximately the same as those in our previous treatment planning studies on BNCT for multiple liver tumors and MPM [5,6]. The details for determination of each parameter have been described in our previous reports [5,6]. The compound biologic effectiveness (CBE) factors of the boron compounds in Table 1 were requested to convert the physical dose of BNCT to the photon-equivalent dose (Gy-Eq) and the relative biologic effectiveness (RBE) of each component of the beam. The CBE factors were used as an alternative RBE in evaluating the biologically equivalent absorbed dose by BNCT. This was because the same or different boron compounds might yield variable effects on different tissues, as a result of variations in the microdistribution of the boron compounds and the morphological character of the target cells. The CBE factors and RBE values for the tumors were the same as those used in clinical BNCT trials [14,15]. The CBE factors and RBE values for liver and lung were determined by experimental studies using rodents [16,17]. We adopted the value of 3.0 as the RBE value of ^{14}N (n,p) ^{14}C radiations and fast neutrons for liver. The value was greater than the RBE of fast neutron for hepatocytes reported by Ono et al. [18]. Use of the greater RBE for normal liver is expected to decrease the occurrence of radiation-induced liver disease in clinical situation.

The difference in the method between BNCT for multiple liver tumors and MPM was the drug delivery system (DDS) for the boron compounds. In BNCT for multiple liver tumors, borocaptate sodium (BSH), which has been employed as a boron compound in clinical BNCT trials for malignant glioma, was administered via the hepatic artery with vessel occlusion materials (lipiodol), according to our previous reports [3,5,7]. This DDS method is possible to deliver ^{10}B to liver tumors, that are highly selective [3]. In the present study, ^{10}B tumor/liver concentration ratio was assumed to be 20 according to our present study (Table 1) [3]. In BNCT for MPM, boronophenylalanine (BPA), another boron compound available in clinical trials, was administered intravenously [8]. In the MPM cases, ^{10}B tumor/lung or liver concentration ratio was assumed to be 3.5 (Table 1).

In BNCT for multiple liver tumors, the whole liver was defined as the clinical target volume (CTV). Three-port irradiation by anterior, right and posterior (ARP) beams was planned to deliver thermal neutrons to whole liver as homogeneously as possible [5]. Because the CTV for MPM was defined as the hemithorax, including the tumor and ipsilateral normal lung, the CTV was divided into upper and lower portions because of the limit in circular collimator size (maximum 25 cm). Each CTV was irradiated with anterior–posterior (AP) beams or 20–30° anterior-oblique and posterior-oblique beams. The oblique beams were used to deliver greater doses to the tumors at mediastinal side compared to AP beams in some cases. Four-port irradiation was needed for covering the whole CTV.

Table 1
^{10}B concentrations and RBE and CBE factors used for conversion of physical dose (Gy) to photon-equivalent dose (Gy-Eq).

	Liver tumor	MPM	Liver	Lung
^{10}B concentration (ppm)	200.0	84.0	10.0 (Liver tumor cases) 24.0 (MPM cases)	24.0
RBE, CBE				
^{10}B (n,a) ^{7}Li	2.5 ($CBE_{for\ BSH}$)	3.8 ($CBE_{for\ BPA}$)	0.94 ($CBE_{for\ BSH}$)* 4.25 ($CBE_{for\ BPA}$)*	2.3 ($CBE_{for\ BPA}$)†
^{14}N (n,p) ^{14}C	3.0	3.0	3.0	2.2†
Fast neutron	3.0	3.0	3.0	2.2†
γ-Ray	1.0	1.0	1.0	1.0

Abbreviations: RBE = relative biological effectiveness; CBE = compound biological effectiveness; MPM = malignant pleural mesothelioma; BSH = borocaptate sodium; BPA = boronophenylalanine.
* Data from Suzuki et al. [16].
† Data from Kiger et al. [17].

Overview of BNCT treatment planning using the simulation environment for radiotherapy applications (SERA) system

Computed tomography (CT) images of four patients with multiple liver tumors and six with MPM were used in the present study. Three patients had right MPM, and the other three had left MPM. In four BNCT treatment plans for multiple liver tumors, a total of 11 liver tumors were evaluated.

We have already reported the treatment planning studies on BNCT for multiple liver tumors and MPM using KUR epi-thermal neutron beam data and the SERA system, a currently available BNCT treatment planning system. Details of the procedures in treatment planning using the SERA system have been described in our previous reports [5,6].

Dose–volume histogram (DVH) analysis

The SERA system can provide DVH data for each tumor or for the normal tissues as a whole. The maximum, minimum and mean doses to the tumors and normal tissues were assessed for each case. In radiotherapy for liver tumors and MPM, radiation-induced liver injury and radiation pneumonitis are dose-limiting toxicities, therefore, we set the doses delivered to normal liver and lung tissues as constraint doses. In the present study, 5.0 Gy-Eq of the mean liver and lung doses were set as the constraint doses. Under these conditions, each DVH parameter and irradiation time was compared between AB-BNCT and RB-BNCT. The doses delivered to the tumors with AB-BNCT and RB-BNCT were compared by means of Wilcoxon's signed-rank test.

Results

Neutron spectra comparison

Fig. 2 shows the neutron spectra at the output port produced by the accelerator-based neutron beam (1 mA, 30 MeV proton beam with the beryllium target) and epi-thermal neutron beam of HWNIF in the KUR. The neutron beam produced by the accelerator was harder compared with that of the KUR. In comparison of the maximum numbers yielded per lethargy, the accelerator source produced neutrons approximately four orders of magnitude higher than KUR.

Comparison of dose distributions in BNCT for multiple liver tumors

Table 2 summarizes the DVH parameters for tumor and normal liver and irradiation time for three-port irradiation in AB-BNCT and RB-BNCT for multiple liver tumors. To compare irradiation time and dose distribution in tumors between AB-BNCT and RB-BNCT, all treatment plans were normalized to deliver mean doses of 5 Gy-Eq to the whole liver. The average irradiation time was 43.8 and 198.3 min in AB-BNCT and RB-BNCT, respectively. The averages of the maximum, mean and minimum doses delivered to all 11 tumors in the AB-BNCT were significantly higher than those in RB-BNCT (78.7 vs. 77.4 Gy-Eq, 68.1 vs. 65.1 Gy-Eq and 57.7 vs. 53.7 Gy-Eq, $p = 0.0023$, $p = 0.0040$, and $p = 0.0022$, respectively).

Fig. 3A shows the isodose distributions in the representative case with deep-seated liver tumor provided by RB-BNCT and AB-BNCT. AB-BNCT delivered higher dose to the tumor than RB-BNCT. Fig. 3B shows the depth–dose distribution profiles along the right

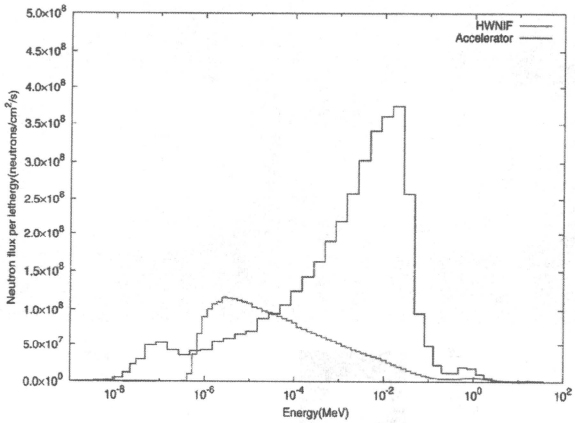

Fig. 2. Comparison of neutron spectrum between HWNIF and accelerator-based neutron source shaped with the BSA.

neutron beam axis which passed into the deep-seated liver tumor. The depth–dose profiles in the tumor located at a depth of 9.0–12.5 cm demonstrated that AB-BNCT delivered a higher dose than RB-BNCT. Fig. 3C shows the depth-ratio of thermal neutron fluence-rate (AB-BCNT to RB-BNCT) profiles along the same beam axis as in Fig. 3B. The ratio of thermal neutron fluence-rate increased from 3.9 to 6.3 at a depth of 1–12 cm, which was caused by the property of the accelerator-based neutron source which has a peak at higher energy in its neutron spectrum compared with that of the KUR as shown in Fig. 2.

Comparison of treatment parameters in BNCT for MPM

Table 3 compares the DVH parameters for tumor and normal lung and irradiation time for four-port irradiation in AB-BNCT and RB-BNCT for MPM. To compare irradiation time and dose distribution in the tumor between AB-BNCT and RB-BNCT, all treatment plans were normalized to deliver mean doses of 5 Gy-Eq to the whole of the ipsilateral lung. The average irradiation time in AB-BNCT and RB-BNCT were 29.9 and 134.7 min, respectively. The mean doses delivered to the MPM tumors by AB-BNCT and RBNCT were 20.2 and 19.9 Gy-Eq, respectively. The average of the maximum doses delivered to the MPM tumors by AB-BNCT was significantly lower than those with RB-BNCT (36.4 vs. 40.0 Gy-Eq, $p = 0.0253$). On the other hand, the average of the minimum doses delivered to the MPM tumors by AB-BNCT was significantly higher than those with RB-BNCT (4.6 vs. 4.3 Gy-Eq, $p = 0.0275$).

Fig. 4A shows the isodose distributions for the tumor in the representative case with MPM provided by RB-BNCT and AB-BNCT. AB-BNCT delivered higher dose to the MPM tumor located in the middle of the thorax compared to RB-BNCT. Fig. 4B shows the depth–dose distribution profiles along the anterior epi-thermal neutron beam axis in the case of MPM. The tumor located at a depth of 9.0–12.5 cm received a greater dose with AB-BNCT compared with RB-BNCT. On the other hand, RB-BNCT delivered a greater dose to the tumor located at a depth of 3.5–5.0 cm. Fig. 4C shows the depth–thermal neutron flux ratio (AB-BCNT to RB-BNCT) profiles along the same beam axis as Fig. 4B. The thermal neutron flux ratio increased from 4.0 to 5.8 within a depth of 1–12 cm.

Discussion

In BNCT for multiple liver tumors and MPM, the most important feature of the AB-BNCT system at our institute is capability to deliver three- or four-port irradiation within a reasonable treatment time (<1 h), including the time required for changing patient position. Shortening of irradiation time makes it possible to finish irradiation while maintaining a high ^{10}B concentration in the tumor, and to reduce the non-selective background dose. In addition, shortening of irradiation time provides comfort to the patients during irradiation and single or two-fractionated BNCT has economic benefits.

Another important feature of the AB-BNCT system is its capability of delivering greater doses to deep-seated tumors than RB-

Table 2
Irradiation time and DVH parameters showing averages (with range) for liver tumors and normal liver.

Neutron source	Irradiation time (min)	Tumor			Liver		
		D_{max} (Gy-eq)	D_{mean} (Gy-eq)	D_{min} (Gy-eq)	D_{max} (Gy-eq)	D_{mean} (Gy-eq)	D_{min} (Gy-eq)
KUR	198.3 (177.0–216.8)	77.4 (49.3–104.6)	65.1 (33.8–84.2)	53.7 (20.7–76.5)	6.9 (6.4–7.4)	5.0*	1.9 (1.3–2.1)
Accelerator	43.8 (39.0–47.8)	78.7 (52.6–102.0	68.1 (37.7–87.1)	57.7 (23.6–76.7)	6.7 (6.3–7.2)	5.0*	1.7 (1.1–2.2)

Abbreviations: DVH = dose-volume histogram; KUR = Kyoto University Research Reactor.
* The mean dose to the liver normalized to 5.0 Gy-Eq.

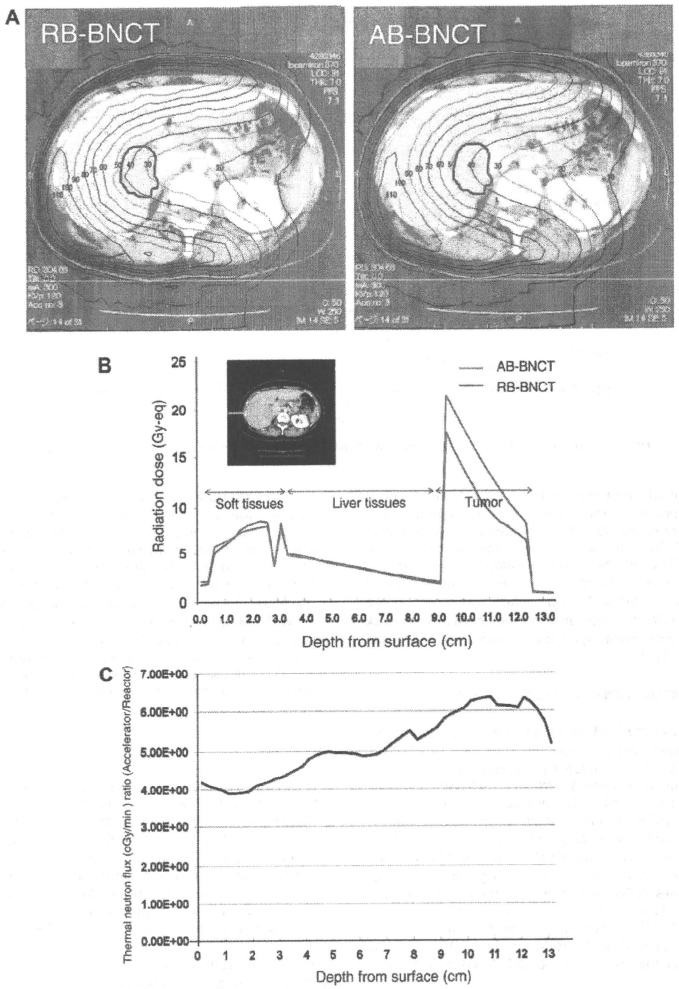

Fig. 3. (A) Comparison of isodose distribution between RB-BNCT and AB-BNCT. The liver tumor is contoured with a solid red line. (B) Depth–dose distribution profiles along the right neutron beam axis, which passed into the deep-seated liver tumor located at a depth of 9.5–12.5 cm. A yellow arrow on the CT image indicates the beam axis. (C) Depth–thermal neutron flux ratio (AB-BCNT to RB-BNCT) profiles along the same beam axis as that in (B).

BNCT, under conditions in which the mean doses delivered to normal liver or lung are equal. This advantage of AB-BNCT over RB-BNCT was especially evident in BNCT for deep-seated multiple liver tumors. As shown in Table 2, AB-BNCT delivered significantly greater doses to liver tumors than RB-BNCT did. As shown in Fig. 2, the AB-BNCT system provided a higher peak energy (near 10 keV) in its neutron spectrum compared with RB-BNCT. The higher energy peak of the AB-BNCT system is well suited for generating a thermal neutron flux distribution suitable for deep-seated tumors and provides a larger thermal neutron fluence to areas deep within the body compared to the RB-BNCT system. However, while the epi-thermal neutron beam of HWNIF in the KUR has a softer spectrum and the near-10-keV component is not significant, the higher epi-thermal neutron component

Table 3
Irradiation time and DVH parameters showing averages (with range) for MPM tumors and normal lung.

Neutron source	Irradiation time (min)	Tumor			Ipsilateral lung			Contralateral lung			Liver*		
		D_{max} (Gy-eq)	D_{mean} (Gy-eq)	D_{min} (Gy-eq)	D_{max} (Gy-eq)	D_{mean} (Gy-eq)	D_{min} (Gy-eq)	D_{max} (Gy-eq)	D_{mean} (Gy-eq)	D_{min} (Gy-eq)	D_{max} (Gy-eq)	D_{mean} (Gy-eq)	D_{min} (Gy-eq)
KUR	134.7 (117.4–156.4)	40.0 (35.0–42.3)	19.9 (19.3–20.7)	4.3 (3.0–6.1)	7.7 (7.1–8.1)	5.0†	2.2 (1.8–2.5)	5.3 (4.7–6.8)	1.4 (1.2–1.9)	0.4 (0.3–0.6)	10.4 (10.0–10.8)	5.0 (4.6–5.2)	0.9 (0.8–1.0)
Accelerator	29.9 (26.3–33.3)	36.4 (33.0–38.3)	20.2 (19.7–21.0)	4.6 (3.4–6.4)	7.3 (6.9–7.5)	5.0†	2.3 (1.8–2.6)	4.9 (4.2–6.0)	1.3 (1.1–1.8)	0.3 (0.2–0.5)	9.7 (9.2–10.2)	5.0 (4.7–5.2)	0.8 (0.7–0.8)

Abbreviations: DVH = dose-volume histogram; MPM = malignant pleural mesothelioma; KUR = Kyoto University Research Reactor.
* The average (range) of DVH data for liver was estimated using the data for three cases with right MPM.
† The mean dose to the liver normalized to 5.0 Gy-Eq.

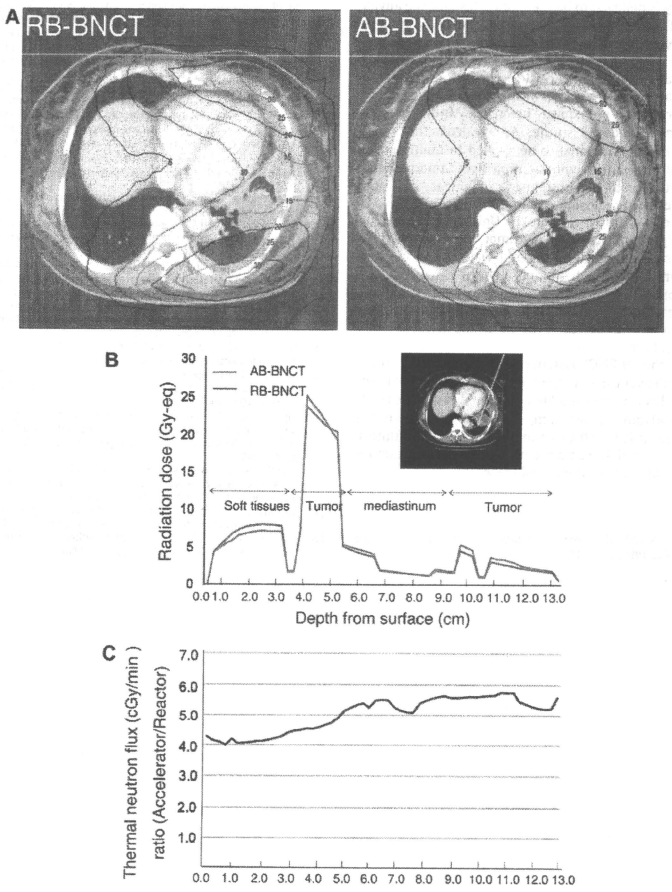

Fig. 4. (A) Comparison of isodose distribution between RB-BNCT and AB-BNCT. (B) Depth–dose distribution profile along the anterior-oblique neutron beam axis in the case of BNCT for MPM. A yellow arrow on the CT image indicates the beam axis. (C) Depth–thermal neutron flux ratio (AB-BCNT to RB-BNCT) profiles along the same beam axis as that in (B).

included in the KUR beam is effective for enlarging the thermal neutron flux at parts deep within the body. This is because the RB-BNCT system can maximize the dose sent to deep-seated tumors near 10 cm, as well as the AB-BNCT system (Figs. 3B and 4B).

Some authors have already reported the advantage of AB-BNCT for deep-seated brain tumors over RB- BNCT using a head phantom. Burlon et al. have reported that AB-BNCT can treat brain tumors that are ~2.0 cm deeper than those treated with RB-BNCT [19]. Blue et al. have reported that, for treatment of brain tumors, compared with RB-BNCT, AB-BNCT can create a neutron field with a significantly better field quality (by a factor of 1.2), which is judged by the dose that can be delivered to a tumor at a depth of 6 cm [20]. The present study is believed to be the first to describe the advantages of AB-BNCT over RB-BNCT in the treatment of body trunk tumors, multiple liver tumors and MPM, apart from brain tumors.

We are preparing to undertake clinical trials with our AB-BNCT system to get an approval as a medical device from the Pharmaceuticals and Medical Devices Agency (PMDA), a Japanese regulatory agency. This approval is a prerequisite before the AB-BNCT system can be constructed at medical institutes. As revealed in the present study, AB-BNCT has the potential to be applied to multiple liver tumors and MPM. The patients with multiple liver tumors, including metastatic tumors or hepatocellular carcinomas, are much greater in number than malignant gliomas or melanomas, which have been treated with BNCT in Japan, the United States and Europe. Selective high-LET irradiation to tumor cells by BNCT has the potential to shed new light on the best way to treat multiple metastatic tumors in lung or brain and pleuritis carcinomatosis. Extending the application of BNCT to many malignancies will lead to further progress in the field of BNCT. After approval of the AB-BNCT system as a medical device, it will be on the market and installed in existing hospitals.

In conclusion, the AB-BNCT system constructed at our institute has the ability to deliver three- or four-port irradiation in the treatment of multiple liver tumors and MPM within a reasonable treatment time (30–60 min). In addition, the AB-BNCT system has advantages over RB-BNCT for the treatment of deep-seated tumors. AB-BNCT has the potential to be a promising treatment option for patients with multiple liver tumors and MPM.

References

[1] Coderre JA, Morris GM. The radiation biology of boron neutron capture therapy. Radiat Res 1999;151:1–18.

[2] Barth RF, Joensuu H. Boron neutron capture therapy for the treatment of glioblastomas and extracranial tumours: as effective, more effective or less effective than photon irradiation? Radiother Oncol 2007;82:119–22.

[3] Suzuki M, Masunaga S, Kinashi Y, et al. Intra-arterial administration of sodium borocaptate (BSH)/lipiodol emulsion delivers B-10 to liver tumors highly selectively for boron neutron capture therapy: experimental studies in the rat liver model. Int J Radiat Oncol Biol Phys 2004;59:260–6.

[4] Suzuki M, Sakurai Y, Masunaga S, et al. Preliminary experimental study of boron neutron capture therapy for malignant tumors spreading in thoracic cavity. Jpn J Clin Oncol 2007;37:245–9.

[5] Suzuki M, Sakurai Y, Masunaga S, Kinashi Y, Nagata K, Ono K. Dosimetric study of boron neutron capture therapy with borocaptate sodium (BSH)/lipiodol emulsion (BSH/lipiodol-BNCT) for treatment of multiple liver tumors. Int J Radiat Oncol Biol Phys 2004;58:892–6.

[6] Suzuki M, Sakurai Y, Masunaga S, et al. Feasibility of boron neutron capture therapy (BNCT) for malignant pleural mesothelioma from a viewpoint of dose distribution analysis. Int J Radiat Oncol Biol Phys 2006;66:1584–9.

[7] Suzuki M, Sakurai Y, Hagiwara S, et al. First attempt of boron neutron capture therapy (BNCT) for hepatocellular carcinoma. Jpn J Clin Oncol 2007;37:376–81.

[8] Suzuki M, Endo K, Satoh H, et al. A novel concept of treatment of diffuse or multiple pleural tumors by boron neutron capture therapy (BNCT). Radiother Oncol 2008;88:192–5.

[9] Lee CL, Zhou XL, Kudchadker RJ, Harmon F, Harker YD. A Monte Carlo dosimetry-based evaluation of the $^{7}Li(p,n)^{7}Be$ reaction near threshold for accelerator boron neutron capture therapy. Med Phys 2000;27:192–202.

[10] Tanaka H, Sakurai Y, Suzuki M, et al. An epithermal neutron generator based on the Be(p,n) reaction using a 30 MeV proton cyclotron accelerator at KURRI. In: Zonta A, Altieri S, Roveda L, Barth R, editors. 13th International Congress on Neutron Capture Therapy "A new option against cancer". Roma: ENEA; 2008. p. 510–3.

[11] IAEA. Current status of neutron capture therapy. In: IAEA TECDOC 1223, Vienna: IAEA; 2001. p. 6–8.

[12] Sakurai Y, Kobayashi T. Controllability of depth dose distribution for neutron capture therapy at the heavy water neutron irradiation facility of Kyoto University Research Reactor. Med Phys 2002;29:2338–50.

[13] Sakurai Y, Kobayashi T. The medical-irradiation characteristics for neutron capture therapy at the heavy water neutron irradiation facility of Kyoto University Research Reactor. Med Phys 2002;29:2328–37.

[14] Kawabata S, Miyatake S, Kajimoto Y, et al. The early successful treatment of glioblastoma patients with modified boron neutron capture therapy. Report of two cases. J Neurooncol 2003;65:159–65.

[15] Kato I, Ono K, Sakurai Y, et al. Effectiveness of BNCT for recurrent head and neck malignancies. Appl Radiat Isot 2004;61:1069–73.

[16] Suzuki M, Masunaga S, Kinashi Y, et al. The effects of boron neutron capture therapy on liver tumors and normal hepatocytes in mice. Jpn J Cancer Res 2000;91:1058–64.

[17] Kiger JL, Kiger WS, Patel H, et al. Functional and histological assessment of the radiobiology of normal rat lung in BNCT. In: Nakagawa Y, Kobayashi T, Fukuda H, editors. Advances in neutron capture therapy 2006. Takamatsu: ISNCT; 2006. p. 85–8.

[18] Ono K, Nagata Y, Akuta K, Abe M, Ando K, Koike S. Frequency of micronuclei in hepatocytes following X and fast-neutron irradiations-an analysis by a linear-quadratic model. Radiat Res 1990;123:345–7.

[19] Burlon AA, Kreiner AJ. A comparison between a TESQ accelerator and a reactor as a neutron sources for BNCT. Nucl Instr Meth Phys Res B 2008;266:763–71.

[20] Blue TE, Yanch JC. Accelerator-based epithermal neutron sources for boron neutron capture therapy of brain tumors. J Neurooncol 2003;62:19–31.

Applied Radiation and Isotopes 67 (2009) S218–S221

Contents lists available at ScienceDirect

Applied Radiation and Isotopes

journal homepage: www.elsevier.com/locate/apradiso

A feasibility study of the post-irradiation dose estimation with SPECT technique for BNCT

Y. Sakurai *, H. Tanaka, M. Suzuki, Y. Kinashi, S. Masunaga, A. Maruhashi, K. Ono

Kyoto University Research Reactor Institute, Asashironishi 2-1010, Kumatori-cho, Sennan-gun, Osaka, Japan

ARTICLE INFO

Keywords:
Post-irradiation dose-estimation
Activation in human body
Radioactivity distribution
Imaging technique
SPECT

ABSTRACT

Various radioactive nuclei are generated in and around the target volume after the irradiation for boron neutron capture therapy. By measuring and estimating the distributions of these nuclei with the technique of single photon emission computed tomography (SPECT), more accurate post-irradiation dose-estimation can be expected. The feasibility study was performed mainly by simulation. The radioactivity densities for Cl-38, Ca-49 and Na-24 just after the irradiation were calculated to be 100–1000 Bq/cm^3 in and around the target volume. It was confirmed that these nuclei could be detected by SPECT under some conditions. Using the density differences for these generated nuclei, discrimination between soft-tissue area and bone area can be achieved. In focusing on the shallower 1 cm^3 voxel, the necessary counting-time for Na-24 was estimated to be a few tens of minutes when the distance between the SPECT detector and the voxel was shortened to 6 cm.

1. Introduction

Since December 2001, at the Heavy Water Neutron Irradiation Facility (HWNIF) of Kyoto University Reactor (KUR) (Sakurai and Kobayashi, 2002), boron neutron capture therapy (BNCT) has been expanded to the tumors of various body parts, such as neck, liver, lung, etc.

The motion ranges and shape changes of these parts are large, unlike those of head. Then, the accuracy is limited in the pre-and post-irradiation dose-estimations by the simulation based on the diagnostic imaging under a motionless and changeless condition.

In BNCT irradiations, various radioactive nuclei are generated in and around the target volume. By measuring and estimating the distributions of these nuclei with the technique of single photon emission computed tomography (SPECT), more accurate post-irradiation dose-estimation can be expected. The feasibility study by simulation calculation is reported.

2. Methods

A dose-estimation code system "SERA" (Wessol et al., 1999) was used in the simulation of the distributions of the radioactive nuclei generated near the target volume. The distributions of the respective radioactive nuclei were calculated using the neutron flux distribution obtained by SERA, with the reaction cross sections in the JENDL-3.3 nuclear data library (Shibata et al., 2002) and decay constants. Here, the physical decrease is taken into account but the biological decrease is not.

The elemental content for some human-tissues important in this study are listed in Table 1 (Synder et al., 1975). The elements important for the activation are sodium (Na), chlorine (Cl), etc., as described below. These are included in the various human tissues at the mass ratio of zero point a few percent.

The radioactivity distributions were simulated for bone, brain and the other soft tissues. The activation of blood is not considered in this estimation, because the simulation of the blood circulation is complicated and difficult. The mass ratios of Na and Cl in blood are almost two times larger than those in soft tissues, and almost the same as those in brain tissue. Assuming that blood is distributed uniformly in the whole body, the mass ratio of blood is a little less than ten percent in each part.

The simulations were performed for the typical BNCT irradiations to brain tumor and head and neck tumor. For the former irradiation, it was assumed that the neutron beam was incident to the parietal lobe and the irradiation time was 1 h. For the latter irradiation, it was assumed that the neutron beam was incident to the right cheek and the irradiation time was 1.5 h. The irradiation field size was 12 cm in diameter for both irradiations.

3. Results

Just after the irradiation, the total radioactivities of the gamma-ray emitting nuclei arranged in order of decreasing

* Corresponding author. Tel.: +81 72 451 2306; fax: +81 72 451 2620.
E-mail address: yosakura@rri.kyoto-u.ac.jp (Y. Sakurai).

0969-8043/$ - see front matter © 2009 Elsevier Ltd. All rights reserved.
doi:10.1016/j.apradiso.2009.03.111

Table 1
Elemental content (mass percent) and density (g/cm^3) for human tissues.

	Bone	Brain	Soft tissue
H	7.19	11.1	10.5
C	25.0	12.5	23.2
N	3.00	1.33	2.49
O	46.9	73.8	63.0
Na	0.32	0.18	0.11
S	0.17	0.18	0.20
P	6.99	0.35	0.13
Cl	0.14	0.24	0.13
K	0.15	0.31	0.20
Ca	9.99	–	–
Density	1.5	1	1

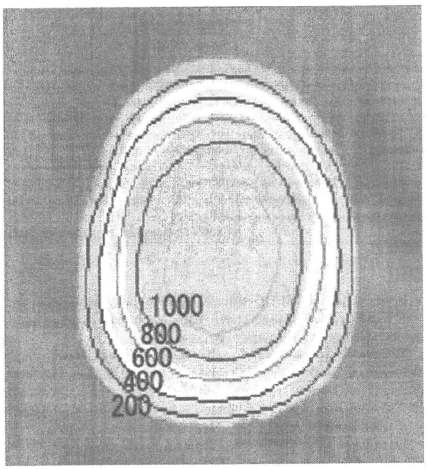

Fig. 1. Contour map for Cl-38 activity density (Bq/cm^3) just after the irradiation to brain tumor.

activity were Cl-38, Na-24 and K-42 in brain and soft tissue both for brain tumor, and head and neck tumor. In bone, the total radioactivities of Ca-49, Na-24, Cl-38 and K-42 were arranged in decreasing order.

Figs. 1–3 are the contour maps for the radioactivity densities on the axial slice at the 3 cm depth just after the irradiation for brain tumor, respectively, for Cl-38, Ca-49 and Na-24. Figs. 4–6 are the contour maps for the radioactivity densities on the beam-line slice just after the irradiation for head and neck tumor. The unit for each contour is Bq/cm^3 in the sample.

In Figs. 1 and 4, the Cl-38 activity density is gently distributed along the beam line. The Cl-38 activity density distributions are relatively similar to the thermal neutron flux distributions. For brain tumor, this is because the density of Cl-37, which is the origin of Cl-38, is almost the same both for bone and brain. For head and neck tumor, this is because the bone area is smaller than the soft-tissue area.

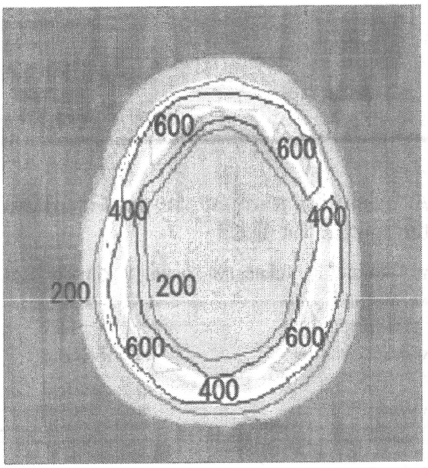

Fig. 2. Contour map for Ca-49 activity density (Bq/cm^3) just after the irradiation to brain tumor.

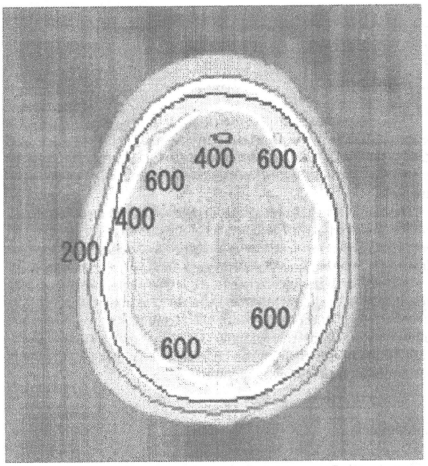

Fig. 3. Contour map for Na-24 activity density (Bq/cm^3) just after the irradiation to brain tumor.

It is found that the Ca-49 activity densities are larger especially in bone, as shown in Figs. 2 and 5. This is because the Ca-48, which is the origin of Ca-49, is distributed mainly in bone.

The Na-24 activity densities are also distributed gently along the beam lines, but the values become larger in bone, as shown in

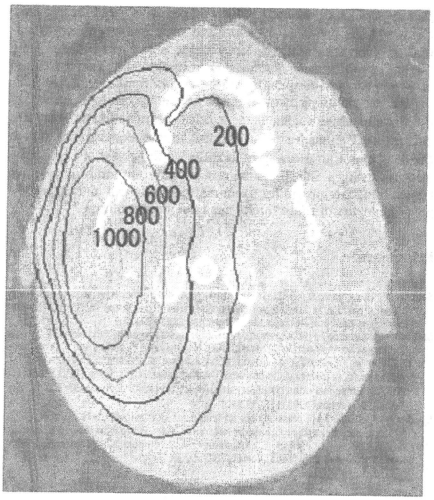

Fig. 4. Contour map for Cl-38 activity density (Bq/cm^3) just after the irradiation to head and neck tumor.

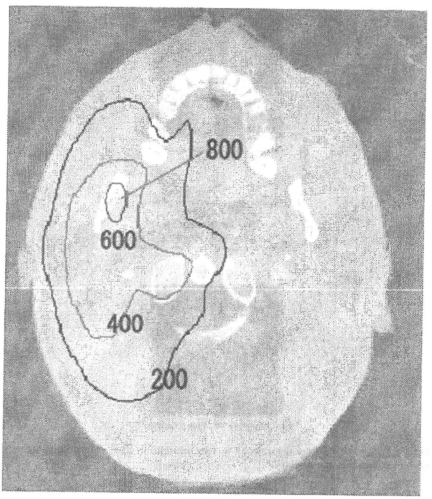

Fig. 6. Contour map for Na-24 activity density (Bq/cm^3) just after the irradiation to head and neck tumor.

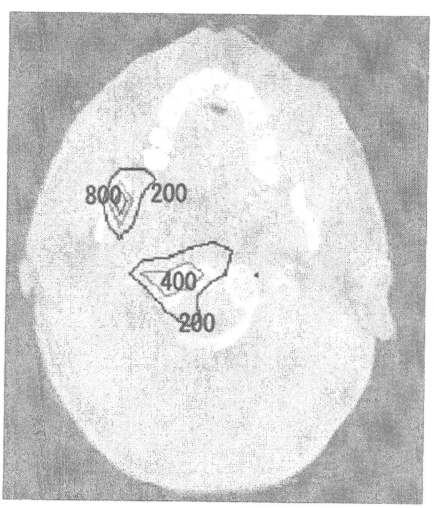

Fig. 5. Contour map for Ca-49 activity density (Bq/cm^3) just after the irradiation to head and neck tumor.

Figs. 3 and 6. This is caused by that the density of Na-23, which is the origin of Na-24, is 2.7 times larger in bone than in brain and soft tissues.

4. Discussion

The radioactivity densities for Cl-38, Ca-49 and Na-24 just after the irradiation were calculated to be in the range from 100 to 1000 Bq/cm^3 in and around the target volume. Cl-38 and Ca-49 decay rapidly after the irradiation, because those half-lives are short, 37 and 8.7 min, respectively. Meanwhile, the half-life of Na-24 is relatively larger at 15 h, so Na-24 can be detected for a few days.

Here, the feasibility of imaging for Na-24 is discussed. For a detector of the SPECT system, it was assumed that the distance to the deepest voxel of 1 cm^3 was 20 cm, and that the effective detection-field size was 1 cm^2. The count rate for the gamma rays from the deepest voxel was estimated to be from 2×10^{-3} to 2×10^{-2} s^{-1}.

To achieve a statistical error of 10%, 1–14 h is necessary. In focusing on the shallower voxel, the necessary counting time was estimated to be a few tens of minutes when the distance between the detector and the voxel was shortened to 6 cm.

A schematic flow diagram of the post-irradiation dose-estimation system with SPECT technique for BNCT is shown in Fig. 7. At present, this system is considered as follows:

(1) From the radioactivity distributions for Ca-49 and Cl-38, the flux distributions of neutrons, mainly thermal neutrons, are obtained, respectively, for the bone and soft-tissue areas.
(2) These flux distributions are compared with the flux distribution obtained from the radioactivity distribution for Na-24.
(3) From the discrepancy between these flux distributions, the effective flux distribution, in which the motion and shape-change near the target volume during the irradiation, is estimated.

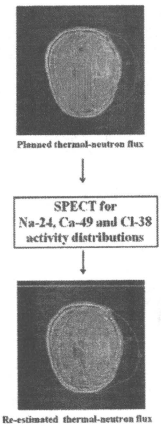

Fig. 7. A schematic flow diagram of the post-irradiation dose-estimation system with SPECT technique for BNCT.

5. Conclusions

It was confirmed that imaging for the Na-24 generated under BNCT could be performed using the SPECT technique. There is a possibility that Ca-49 and Cl-38 could also be utilized for imaging, though those half-lives are short and therefore contain information only for the middle to latter phase of the irradiation. Using the density differences for these generated nuclei, discrimination between the soft-tissue area and bone area can be expected.

We are planning to quantitatively confirm the generation of these radioactive nuclei using a HPGe semiconductor detector, etc., in BNCT clinical irradiations and animal experiments, when the KUR operation is restarted in 2009. We are expecting to try the imaging using a SPECT machine if possible. In addition, we are researching the possibility to model the biological and physiological behaviors of these nuclei near the target volume.

References

Sakurai, Y., Kobayashi, T., 2002. The medical-irradiation characteristics for neutron capture therapy at the Heavy Water Neutron Irradiation Facility of Kyoto University Research Reactor. Med. Phys. 29, 2328–2337.

Shibata, K., Kawano, T., Nakagawa, T., Iwamoto, O., Katakura, J., Fukahori, T., Chiba, S., Hasegawa, A., Murata, T., Matsunobu, H., Ohsawa, T., Nakajima, Y., Yoshida, T., Zukeran, A., Kawai, M., Baba, M., Ishikawa, M., Asami, T., Watanabe, T., Watanabe, Y., Igashira, M., Yamamuro, N., Kitazawa, H., Yamano, N., Takano, H., 2002. Japanese evaluated nuclear data library version 3 revision-3: JENDL-3.3. J. Nucl. Sci. Technol. 39, 1125–1136.

Synder, W.S., Cook, M.J., Nasset, E.S., Kahrhausen, L.R., Howells, G.P., Tipon, L.H., 1975. Report of the Task Group on Reference Man. Pergamon Press, Oxford.

Wessol, D., Cohen, M., Harkin, G., Rossmeier, M., Wemple, C., Wheeler, F., 1999. SERA Workshop Lab Manual, INEEL/EXT-99-00766.

Applied Radiation and Isotopes 67 (2009) S37–S42

Contents lists available at ScienceDirect

Applied Radiation and Isotopes

journal homepage: www.elsevier.com/locate/apradiso

Effectiveness of boron neutron capture therapy for recurrent head and neck malignancies

Itsuro Kato [a,*], Yusei Fujita [a], Akira Maruhashi [b], Hiroaki Kumada [c], Masatoshi Ohmae [d], Mitsunori Kirihata [e], Yoshio Imahori [f,g], Minoru Suzuki [b], Yoshinori Sakrai [h], Tetsuro Sumi [a], Soichi Iwai [a], Mitsuhiro Nakazawa [a], Isao Murata [i], Hiroyuki Miyamaru [i], Koji Ono [b]

[a] Department of Oral and Maxillofacial Surgery, II Osaka University, Graduate School of Dentistry, Osaka, Japan
[b] Radiation Oncology Research Laboratory, Research Reactor Institut, Kyoto University, Osaka, Japan
[c] Japan Atomic Energy Agency, Tokai Research and Development Center, Ibaraki, Japan
[d] Department of Oral and Maxillofacial Surgery, Izimisano Municipal Hospital, Rinku General Hospital, Izumisano, Osaka, Japan
[e] Graduate School of Environment and Life Science, Osaka prefectural University, Osaka, Japan
[f] Department of Neurosurgery, Kyoto Prefectural University, Kyoto
[g] CEO of Cancer Intelligence Care Systems, Inc., Tokyo, Japan
[h] Graduate School of Medicine, Sapporo Medical University of Medicine, Hokkaido, Japan
[i] Division of Electrical, Electronic and Information Engineering, Graduate School of Engineering, Osaka University, Japan

ARTICLE INFO

Keywords:
Head and neck cancer
BNCT
Epithermal neutron
BPA
BSH

ABSTRACT

It is necessary to explore new treatments for recurrent head and neck malignancies (HNM) to avoid severe impairment of oro-facial structures and functions. Boron neutron capture therapy (BNCT) is tumor-cell targeted radiotherapy that has significant superiority over conventional radiotherapies in principle.

We have treated with BNCT 42 times for 26 patients (19 squamous cell carcinomas (SCC), 4 salivary gland carcinomas and 3 sarcomas) with a recurrent and far advanced HNM since 2001. Results of (1) ^{10}B concentration of tumor/normal tissue ratios (T/N ratio) of FBPA-PET studies were SCC: 1.8–5.7, sarcoma: 2.5–4.0, parotid tumor: 2.5–3.7. (2) Therapeutic effects were CR: 12 cases, PR: 10 cases, PD: 3 cases NE (not evaluated): 1 case. Response rate was 85%. (3) Improvement of QOL such as a relief of severe pain, bleeding, and exudates at the local lesion, improvement of PS, disappearance of ulceration, covered with normal skin and preserved oral and maxillofacial functions and tissues. (4) Survival periods after BNCT were 1–72 months (mean: 13.6 months). Six-year survival rate was 24% by Kaplan–Meier analysis. (5) Adverse-events were transient mucositis and alopecia in most of the cases; three osteomyelitis and one brain necrosis were recognized. These results indicate that BNCT represents a new and promising treatment approach for advanced HNM.

1. Introduction

Head and neck cancers are the sixth prevalent cancer in the world, with a global yearly incidence of 500,000. Although modest gains in local control and survival have been achieved with appropriate use of surgical intervention combined with radiation therapy and chemotherapy, in the last 20 years, 5-year survival rates for head and neck malignancies (HNM) have not improved significantly, remaining at 52% (Smith and Haffty, 1999). HNM are often radio- and chemo-resistant, necessitating a wide resection including the surrounding tissues, which results in severe impairment of oro-facial structures and functions. In this context, it is necessary to explore new applications for a full assessment of Boron neutron capture therapy (BNCT) which may well benefit HNM. So we had started basic research used human- and murine-squamous carcinoma cell lines (Obayashi et al., 2004; Kamida et al., 2006) as well as other animal experimental model (Kreimann et al., 2001).

BNCT is a binary cancer treatment modality that involves the selective accumulation of ^{10}B carriers in tumors followed by irradiation with a epithermal neutron beam. The high energy transfers α particles and recoiling ^{7}Li nuclei emitted during the capture of a thermal neutron in the ^{10}B (n, α) ^{7}Li reaction which carry an average total kinetic energy of 2.34 MeV, and have a short range (4–9 μm) of approximately one cell diameter, resulting in induction of a large relative biological effectiveness and selective destruction of tumor cells containing ^{10}B. The clinical application of BNCT has been limited to advanced brain tumor (Slatkin, 1991;

* Corresponding author. Tel.: +81 6 687 92 941; fax: +81 6 6879 2170.
E-mail address: katoitsu@dent.osaka-u.ac.jp (I. Kato).

0969-8043/$ - see front matter © 2009 Elsevier Ltd. All rights reserved.
doi:10.1016/j.apradiso.2009.03.103

Nakagawa and Hatanaka, 1997) and malignant melanomas (Mishima et al., 1989). We, first in the world, reported six patients with HNM who have been treated with BNCT (Kato et al., 2004). The clinical phases I and II trial of BNCT was recently reported (Kankaanranta et al., 2007). The purpose of this study is to estimate of safety and efficacies of BNCT. We report here clinical results and outcome of 26 patients with HNM, who have been treated with BNCT in the Kyoto University Research Reactor Institute (KUR) and at Japan Atomic Energy Agency (JAEA) Reactor, JRR4 from December 2001 to December 2007.

2. Materials and methods

2.1. Patients

The 26 patients with HNM were 19 squamous cell carcinomas (SCCs), 4 salivary gland carcinomas and 3 sarcomas. All the patients but one had received standard therapy and had developed recurrent HNM for which there were no other treatment options. All the cases had the approval of the ethical committees, medical committee of KUR and that of Osaka University, Graduate School of Dentistry. Characteristics of 26 cases were summarized in Table 1.

2.2. ^{18}F-BPA PET study

The accumulation of BPA to tumor and normal tissue was imaged and quantified by ^{18}F-BPA-PET study before BNCT. The synthesis method and preparation of L-^{18}F-BPA and the choice of region of interests (ROIs) are detailed in our previous report (Kato et al., 2004).

2.3. Boron compounds

A combination of borocaptate sodium (BSH) and *para*-boronophenylalanine (BPA) were administered intravenously (i.v.) as ^{10}B-carriers in the first 13 times of BNCT in 10 cases (Table 1) (Ono et al., 1999). The administration methods were written in the previous reports (Kato et al., 2004). BPA (250 mg/kg body weight) in fructose solution were administered intravenously for 1 h. The epithermal neutron irradiation with KUR was started 12 and 1 h after the administration of BSH and BPA, respectively. In the rest of 16 cases, BPA (250 or 500 mg/kg body weight) alone was administered for 1 or 2 h, respectively, followed by the epithermal neutron irradiation.

2.4. Measurement of neutron fluence, ^{10}B-concetration and dose estimation

The distributions of neutron fluences, the physical doses of neutrons and gamma-rays were calculated by the dose-planning system "SERA" at KUR and "JCDS" at JAEA. Details of estimation methods of neutron fluence, ^{10}B concentration and CBE and RBE-weighted doses were written in the previous reports (Kato et al. (2004)).

3. Results

The results of all 26 cases are summarized in Table 1. Most of the 26 cases were recurrent and far advanced HNM such as 15 out of 26 cases (58%) developed regional lymph node metastases and 6 out of 15 cases (40%) with lymph nodes metastases developed distant metastases.

So far for 6 years, we have treated with BNCT 42 times for 26 patients with a recurrent HNM since 2001. Results are as follows. (1) ^{10}B concentration of tumor/normal tissue ratios (T/N ratio) of PET studies were SCC: 1.8–5.7, sarcoma: 2.5–4.0, parotid tumor: 2.5–3.7. (2) Regression rates were CR: 12 cases (46%), PR: 10 cases (39%), PD: 3 cases (12%), NE (not evaluated): 1 case. Response rate was 85%. Nine patients (35%) were disease free survival. (3) BNCT improved QOL, PS and survival periods. (4) Survival periods after BNCT were 1–72 months (mean: 13.6 months). Six-year survival rate was 24% by Kaplan–Meier analysis shown in Fig. 1. (5) Adverse-events were brain necrosis, osteomyelitis and transient mucositis and alopecia. Aphasia owing to the brain edema and necrosis in case 1 had been transiently recovered, after treated with massive dose therapy of vitamin E and steroid hormone.

Typical cases which had been treated with BNCT are written here for the clinical course of a disease.

Case 1: *5 times of BNCT has brought a patient with recurrent huge cancer disease free and long survival*: A 67-year-old woman was diagnosed as muco-epidermoid carcinoma (MEC) of parotid gland in 1998 and underwent a parotidectomy, followed by 45 Gy of radiation therapy. In March 1999 the tumor had recurred and additional chemotherapy was ineffective. In October 2001 the ulcerated tumor had grown to 13.5 × 12.5 × 8 cm, which caused severe pain, bleeding and mucous exudates.

The first BNCT was performed using epithermal neutron in KUR under the administration of both BSH (5 g) and BPA (250 mg/kg) in December 2001. Although the tumor had shrunk to 63% during 1 month, the surface of the tumor had partially re-grown; we decided to perform the second BNCT, seated 5 mm thickness gelatin-sheet on surface of the tumor in order to compensate insufficient radiation dose at the tumor surface. The huge tumor had gradually shrunk to 18% of the size of the original during 1-year with relief of pain, decrease of exudates-secretion from the ulcer, disappearance of tumor ulceration and being covered with normal skin. As the tumor still had partially remained at retroauricular and subauricular portion, the third BNCT with 5 mm thickness gelatin-sheet was performed in a sitting posture to set up the tumor closely to the collimator of KUR in December 2002. The tumor had shrunk to 6% and had remained the same size for about 3 years (Kato et al., 2004). In November 2005, the left neck had suddenly begun to swell with pain, tenderness and redness, PET-CT revealed that tumor had re-grown. The fourth and fifth BNCT had undergone in December 2005 and January 2006, respectively, in KUR. The recurrent cervical tumor had gradually disappeared; however, cervical skin defect had developed in April 2006. In August 2006, internal carotid artery had suddenly ruptured and she was transported to the ICU, which she could escape death. She has been disease free survival for 72 months.

Case 9: *BNCT for a carcinoma which developed favorably nerve invasion in case of residual tumor after operation*: A 61-year-old woman with a residual maxillary cancer infiltrating into pterygopalatine fossa (T4N1M0, adenoid cystic carcinoma) after maxillectomy was treated with 2 times of BPA mediated-BNCT in September and October 2004 (Fig. 2A). In the first BNCT, BPA 250 mg/kg was administered intravenously and in the second BNCT, BPA 250 mg/kg was administered intra-arterially (ia). T/N ratio of ^{10}B concentration was 2.5 and 7.6, respectively. A peak of RBE, CBE-weighted total absorbed dose at the deepest tumor (7 cm depth) was 14 Gy-Eq in the first and that at deepest tumor (5.5 cm depth) was 30 Gy-Eq in the second BNCT. A peak at normal membrane was 11.6 Gy-Eq in the first and was 7.8 Gy-Eq in the second BNCT, respectively. A residual maxillary cancer and regional lymph node metastasis were disappeared about 7 months after 2 times of BNCT was followed by the chemotherapy (THP-ADR 30 mg ia, CDDP 48 mg, CPA 480 mg iv) as shown in Fig. 2B. The primary tumor remains unseen for so far

Table 1
Treatment summary of 26 cases treated with BNCT.

Case	Gender	Age	No.	Boron compounds		Histopathological diagnosis	History		Longest	T/N ratio	OB conc. (ppm)	Irradiation time (min)	Criteira for irradiation time	Adverse event		% Volume of original (months)	Survival (month)	Prognosis	Remarks
				BSH/ Body	BPA/kg		RT(Gy)	Ope Y/N	Diameter (cm)		Mean		DT: deepest tumor, M: mucosa, S: skin, N: normal	Mucositis NCI-CTC	Others				
1	F	67	1	5 g	250 mg	MEC	50	Y	13.5	3.3	24.8+14.4	60	(DT22.9 Gy•S5.5 Gy)	<2		63%(1)			
			2	5 g	250 mg						23+14	75	DT28 Gy•S5.2 Gy)	<2		18%(11)		Disappearance of ulcer	
			3	5 g	250 mg					3.5	27+7.14	90	(DT10 Gy•S5 Gy)	<2	OM	6%(17)			No change in size for 34-months regrowth
			4	(−)	500 mg					3.3	25	75	DT25 Gy•(M17.5 Gy)	<2	Brain necrosis				
			5	(−)	500 mg					3.3	25	90→75	M16 Gy (DT16Gy)→ 13.3 Gy	<2			72	Alive	
2	M	61	1	5 g	250 mg	Oateosarcoma	68	Y	10.0	4.0		40		<2		46%(6)	8	DOC	PS:4→PS:2
3	M	56	1	5 g	250 mg	SCC	70	Y	4.0	1.8	35.4+12	120	(DT21.5 Gy•S8 Gy)	<2		PD	10	DOC	
4	F	60	1	5 g	250 mg	SCC	No	Y	11.0	4.4	50+11.4	77	(DT5.7 Gy•S5 Gy)	<2		27%(1)	1	DOC	Disappearance of pain
5	M	73	1	5 g	250 mg	SCC	60	Y	8.0	4.0	35+11.3	100	DT36.5 Gy (S7.1 Gy)	<2	OM	CR	7	DOI	Distant. meta.
6	M	51	1	5 g	250 mg	SCC	No	Y	8.0	4.6	16.3+12	120	DT12.2 Gy (N6.8 Gy)	<2		NE	5	DOC	Distant. meta.
7	F	58	1	5 g	250 mg	IPS	50	Y	7.0	3.1	23.6+12	120	DT14.4 Gy (M6.1 Gy)	<2		17%(1.5)		Prevent eye ball from removing	
			2	5 g	250 mg					3.1	26.6+12	120	DT20 Gy (N8.9 Gy)	<2		8%(9)	31	Alive	Recurrence
8	M	53	1	(−)	250 mg	MEC	No	Y	8.0	2.8	12	114	DT5.7 Gy•(N4.7Gy)	<2		8%(3)	3	DOC	Distant. meta.
9	F	61	1	(−)	250 mg	ACC	No	Y	4.0	2.5	15.5	100	DT14 Gy (M11.6 Gy)	<2		6%(1.5)		Shrinkage of meta. LN	
			2	(−)	250 mg	IA			1.5	7.6[a]	22.3	66	DT30 Gy (M7.8 Gy)	<2		CR	39	Alive	Distant. meta.
10	F	51	1	5 g	250 mg	SCC	No	Y	8.0	3.1	29+12	90	DT15 Gy (M12.2 Gy)	<2		10%(1.5)	3	DOI	
			2	(−)	250 mg	IA			4.0	4.3[a]	15	60	DT12 Gy (M7 Gy)	<2					
11	F	77	1	5 g	250 mg	SCC	51	Y	5.0	4.4	30.3+11.4	51	M13 Gy (DT34 Gy)	<2		<5%(1)		Shrinkage of meta. LN	
			2	(−)	500 mg				2.5		24	60	DT20 Gy (M8.6 Gy)	<2			6	DOC	Distant. meta.
12	M	78	1	(−)	500 mg	SCC	54	Y	4.0	4.4	24.0	82	DT20 Gy (M10.8 Gy)	<2		<5%	34	Alive	
			2	(−)	500 mg	C-IV			2.0		25.0	60	DT 20Gy (M10.6 Gy)	<2				Third primary carcinoma	
13	M	75	1	5 g	500 mg	SCC	45	Y	4.5	2.0	35.4+24	73	DT20 Gy (M10.9 Gy)	3		CR	14	DOC	
			2	(−)	500 mg	C-IV			1.5		24.0	90	M12 Gy (DT18Gy)	3				Recurrence of meta. LN	
			3	(−)	500 mg				2.0		22.0	90	(DT5.9 Gy, M7.0 Gy)	3		CR			
14	M	59	1	(−)	250 mg[a]	Angiosarcoma	No	Y	3.0	2.5	15.0[a]	60	M15 Gy(DT10.8 Gy)	<2		CR	30	Alive	
			2	(−)	500 mg				3.0		24.0	45	M15 Gy (DT11.3Gy)	<2				Treated as adjuvant therapy	
15	M	35	1	(−)	500 mg	IA SCC	85	N	9.0	3.5	IA55	33	M15 Gy (DT6 · 20 Gy)	<2		PD	2	DOC	
16	M	56	1	(−)	500 mg	MEC	No	Y	0.9	3.7	25.3	60	M12 Gy•DT22 Gy	<2		CR	27	Alive	Rouviere's LN Meta.
17	M	63	1	(−)	500 mg	SCC	64	Y	2.0	2.9	25.3	90	DT30 Gy (M15.9 Gy)	4			8	DOC	Distant. Meta (Lung).
			2	(−)	500 mg				1.0			90	M10 Gy (DT18 Gy)	4		<5%			

Table 1 (*continued*)

Case	Gender	Age	No.	Boron compounds			Histopathological diagnosis	History		Longest	T/N ratio	0B conc. (ppm)	Irradiation time (min)	Criteira for irradiation time	Adverse event		% Volume of original	Survival (month)	Prognosis	Remarks
				BSH/ Body	BPA/kg			RT(Gy)	Ope Y/N	Diameter (cm)		Mean		DT: deepest tumor, M: mucosa, S: skin, N: normal	Mucositis NCI-CTC	Others	(months)			
																				Multiple skin metstasis at bilateral neck
18	F	72	1	(−)	500 mg	C-IV	SCC	50	Y	2.0	3.7	24.0	50	DT30 Gy (M12.7 Gy)	4		<5%(1)	8	DOC	Meta. LN
			2	(−)	500 mg	C-IV				5.0	2.4		90	DT30 Gy (M12.7 Gy)	4					
			3	(−)	500 mg	C-IV				5.0	2.4	18.0	120	DT15 Gy	4					
19	M	57	1	(−)	>500	C-IV	SCC	60	Y	7.0	5.7	34.2	60	M15 Gy•DT30 Gy			<5%(1)	7	DOC	Meta. LN
			2	(−)	>500	C-IV				12.0		36.0	40	DT20 Gy (M8.1 Gy)	<2		20%			
20	M	55	1	(−)	500(360)		SCC	67	N	12.0	3.0	11.0[a]	60	DT20 Gy (M8.1 Gy)	<2		PD	1	DOC	Meta. LN
21	F	85	1	(−)	500 mg	C-IV	SCC	74	Y	2.0	2.5	28.7	40	M13 Gy	<2	OM	CR	8	DOC	Colon cancer
22	M	56	1	(−)	500 mg	C-IV	SCC	52	Y	6.8	5.7	30.2	25	D:9.8 (GTV:77, 35 Gy)	<2		CR	9	Alive	Invasion to orbital fossa and frontal lobe
23	F	59	1	(−)	500 mg	C-IV	SCC	64	Y	8.0	3.3	22.4	25	D:9.9 (GTV:27,9.9 Gy)	<2		PR	5	Alive	
24	F	57	1	(−)	500 mg	C-IV	SCC	40+46	Y	4.0	2.9	19.2	35	D:9.3 (GTV:35,17 Gy)	<2		CR	7	Alive	Forth cancer
25	M	47	1	(−)	500 mg	C-IV	SCC	60+35	Y	6.0	3.3	24.2	42	D:10.1 Gy (GTV59.3, 32.8 Gy)	3		CR	5	Alive	
26	M	71	1	(−)	500 mg	C-IV	SCC	60	N	5.7	2.9	27.0	36	D:10 (GTV:40.1,26.9)	<2		CR	3	Alive	disappearance of pain

MEC: mucoepidermoid carcinoma, SCC: squsmoud cell carcinoma, IFS: inflammatory fibrosarcoma, ACC: adenoid cystic carcinoma.

[a] BPA(1A), G:5 mmGelatin, T/N: ^{10}B conc. of Tumor/Normal, M: Male, F: Female, IA: Intra-arterirally, IV: intra-venously, C-IV: continuous IV, PD:progressive disease, CR:complete response, NE:not evaluated, OM: osteomyelitis, DOC: dead from cancer, DOI: death from an intercurrent cause.

42 months although bilateral multiple lung metastases have developed 18 months the after first BNCT.

Case 12: BNCT for third primary carcinoma at head and neck region: A 78-year-old man with a recurrent oro-pharyngeal carcinoma (recurrence of third primary carcinoma) after the treatments for root of tongue carcinoma had no treatment options in January 2005. He had suffered from the left tongue cancer (first primary carcinoma, T1N0M0) and was treated with 70 Gy of interstitial Ir-hair pin radiation therapy in 1980. He was treated with 64 Gy of radiation therapy for laryngeal carcinoma (second primary carcinoma, T1aN0M0) in 1990. In February 2000, tongue carcinoma (third primary carcinoma, T2N1M0) was found and was treated with operation of Lt-Radical neck dissection, hemi-glossectomy, reconstruction of PMMC in March. About 20 mm diameter of recurrent exophytic carcinoma at root of tongue had again excised in May, followed by 54 Gy of external RT in June–July 2003. T/N ratio of ^{10}B concentration was 4.4. A recurrent oro-pharyngeal carcinoma (T1N0M0, SCC) was treated 2 times with BPA mediated-BNCT in February and September 2005 in KUR. Both root of tongue carcinoma and middle pharyngeal carcinoma had disappeared 4 months after BNCT. The patient remains disease free for 34 months so far.

Case 14: Role of BNCT for the treatment of angiosarcoma: A 59-year-old man with the left maxillary gingival to buccal mucosa was diagnosed as angiosarcoma. Histopathological findings of H&E and immunohistochemical sections indicated a network of anastomosing channels and solid areas immunoreactive for CD31 and CD34. So pathologists concluded angiosarcoma. T/N ratio of ^{10}B concentration estimated from FBPA-PET study was 2.5. Human recombinant IL-2 was intra-arterially administered and locally injected for 2 weeks in April 2005. Aggressive growth was stopped and the tumor was not reduced in size; treatment effect was NC. The tumor was removed surgically with 1 cm safety margin in May 2005, followed by 2 times of BNCT in June and July. Three times of immunotherapy just after each BNCT and 1 month after second BNCT were treated as adjuvant therapy. The patient remains disease free for 30 months so far.

Case 16: Role of BNCT for metastatic node of Rouviere in case of high-grade muco-epidermoid carcinoma: A 56-year-old man with the right buccal carcinoma (T4N2bM0, high-grade muco-epidermoid carcinoma) after operation, chemotherapy, developed metastatic node of Rouviere in July 2005. The patient did not choose surgical operation. T/N ratio estimated from FBPA-PET study was 3.7 (Fig. 3A). The patient was treated with BPA mediated-BNCT in September 2005. The lymph node was 5.2 cm depth from skin surface and RBE, CBE-weighted total absorbed dose was 22 Gy-Eq in metastatic node, that in normal membrane was 12 Gy-Eq. FBPA-PET study at 2 months after BNCT showed no accumulation of FBPA (Fig. 3B). The patient remains disease free for 27 months so far.

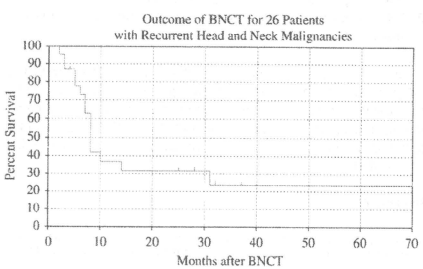

Fig. 1. Six-year survival rate of 26 cases treated with BNCT were 24% by Kaplan–Meier Analysis.

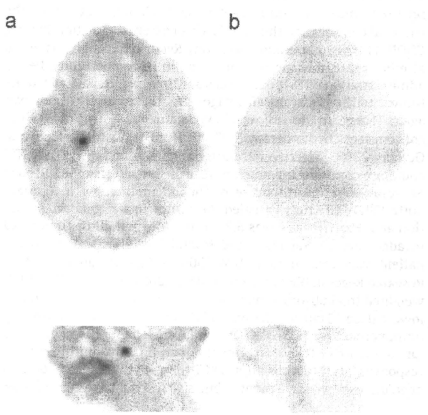

Fig. 3. (A) FBPA-PET-study in case 16 prior to BNCT. FBPA was accumulated in the Rouviere node. (B) 2 months after BNCT. No accumulation in the FBPA-PET 2 months after BNCT.

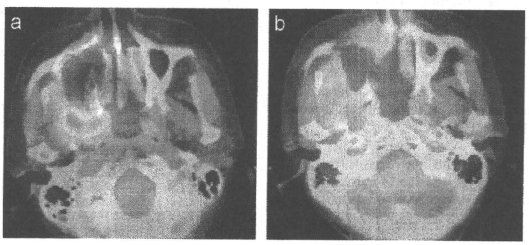

Fig. 2. (A) FBPA-PET study in case 9 prior to BNCT. A residual maxillary cancer (arrow heads) infiltrating into fossa pterygo-palatina (T4N1M0, adenoid cystic carcinoma) after maxillectomy was treated with 2 times of BPA mediated-BNCT followed by the chemotherapy. (B) 7 months after the first BNCT.

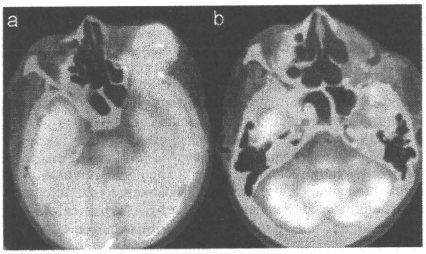

Fig. 4. (A) FDG-PET study in case 22 prior to BNCT. FDG tracer was accumulated in the left orbital region (arrow heads) and frontal lobe of brain. (B) 6 months after BNCT. No accumulation of FDG-PET was recognized 6 months after BNCT.

Case 22: Role of BNCT for advanced maxillary sinus cancer invaded into orbital fossa and frontal lobe: A 56-year-old man with a recurrent maxillary sinus carcinoma (T4N1M0, SCC) after the trimodal combination therapy (52 Gy of external radiationtherapy, CDDP: 113 mg total ia and operation). Recurrent cancer was found at ethmoidal sinus and orbital region in November 2005. Per os administration of TS-1 for 2 weeks and 1 week interval had led the tumor to disappear on MR images. As the recurrent tumor was again found in the inside of zygomatic bone, the multi-drug concomitant chemotherapy (TXT, CDDP, 5Fu) was not effective in October 2006. Selective intra-arterial chemotherapy (CDDP+STS) could not continue anymore because of side effects of CDDP such as dyspnea at fourth course of this chemotherapy in February 2007. FBPA-PET study revealed the cancer had a good accumulation and that T/N ratio was 5.7. During this period the tumor had invaded into orbital fossa and frontal lobe (Fig. 4A). Then the patient was treated with BPA (500 mg/kg)-mediated BNCT in Research Reactor, JRR4 at JAEA in March 2007. A peak of RBE, CBE-weighted total absorbed dose at the mean GTV was 77 Gy-Eq and lowest dose (5 cm depth) was 35 Gy-Eq. BNCT was followed by immunotherapy (CD3-LAK) and adjuvant chemotherapy of TS-1 for 6 months. These treatments had brought him complete response (CR) 6 months after BNCT (Fig. 4B) and he has not only been disease free for 9 months but also he could save his left eye.

4. Conclusions

Treatment modalities for HNM are now mainly limited to surgery, radiotherapy, chemotherapy and their combinations. As there is esthetic preference of patients, which should be considered, it is important for treatment modality to be able to preserve those structures and functions. To avoid severe impairment of oro-facial structures and functions, we had applied BNCT for extended indication of HNM and we could ascertain the effectiveness of BNCT for 22 out of 26 patients with advanced or recurrent HNM for which there were no other treatment options.

Merits of BNCT applying for HNM are as follows:

(1) As there are important structures and functions in the head and neck regions and also there is esthetic preference of patients, it is possible for BNCT to preserve those structures and functions.
(2) As field cancerization and multiple primaries cancers are especially popular in upper aerodigestive tract, it is important for BNCT to preserve those structures and functions in head and neck region.
(3) Patients with a recurrent cancer who had been treated with full dose of radiation therapy could be contraindication for both conventional radiation therapy and the ion-beam therapy, but those who could be indication for BNCT.
(4) For patients with the cancer infiltrating preferably into nerve or bone, it is difficult to be cured to get enough surgical margins, but BNCT makes it possible to be cured because of tumor-selectivity.
(5) Lymph node metastases or skin metastases which are difficult to be removed surgically should be also indication for BNCT.
(6) T/N ratio of ^{10}B concentration estimated from FBPA-PET study could make the patients possible to predict their prognosis to some extent, because the higher the T/N ratio, the better their prognosis will be.
(7) There seemed to be high potential indication for patients with SCC, because their T/N ratios were relatively high such as 1.8–5.7 (mean 3.6).
(8) Even if a tumor is radiation-insensitive or chemotherapy-insensitive, enough accumulation of ^{10}B in the tumor tissues should be expected to be good prognosis.
(9) BNCT is less-invasive treatment modality compared with surgical operation.

Demerits of BNCT applying for HNM are as follows:

(1) As neutron source now depends on research reactor, patients have to go to Research Reactor for BNCT.
(2) BNCT is not so effective for deep-seated tumor more than 6 cm from surface of the skin.

We are now under construction of the accelerator for BNCT. Many researchers are now investigating new boron compounds, drug delivery systems, administration methods for boron compounds and so on. These results indicated that BNCT represents a new and promising treatment approach even for a huge or far advanced HNM.

References

Kamida, A., et al., 2006. Effects of boron neutron capture therapy on human oral squamous cell carcinoma in a nude mouse model. Int. J. Radiat. Biol. 82 (1). 21–29.
Kankaanranta, L., et al., 2007. Boron neutron capture therapy in the treatment of locally recurred head and neck cancer. Int. J. Radiat. Oncol. Biol. Phys. 69, 475–482.
Kato, I., et al., 2004. Effectiveness of BNCT for recurrent head and neck malignancies. Appl. Radiat. Isot. 61, 1069–1073.
Kreimann, E.L., Itoiz, M.E., et al., 2001. Boron neutron capture therapy for the treatment of oral cancer in the hamster cheek pouch model. Cancer Res. 6, 8638–8642.
Mishima, Y., et al., 1989. Treatment of malignant melanoma by single thermal neutron capture therapy with melanoma-seeking ^{10}B-compound. Lancet 39, 325–333.
Nakagawa, Y., Hatanaka, H., 1997. Boron neutron capture therapy: clinical brain tumor studies. J. Neurooncol. 33, 105–115.
Obayashi, S., et al., 2004. Delivery of 10 boron to oral squamous cell carcinoma using boronophenyl-alanine and borocaptate sodium for boron neutron capture therapy. Oral Oncol. 40, 474–482.
Ono, K., et al., 1999. The combined effect of boronophenylalanine and borocaptate in boron neutron capture therapy for SCCVII tumors in mice. Int. J. Radiat. Oncol. Biol. Phys. 43, 431–466.
Slatkin, D.N., 1991. A history of boron neutron capture therapy of brain tumors. Postulation of a brain radiation dose tolerance limit. Brain 114, 1609–1629.
Smith, D., Haffty, B.G., 1999. Radiat. Oncol. Invest. 7, 125–144.

Applied Radiation and Isotopes 67 (2009) S15–S18

Contents lists available at ScienceDirect

Applied Radiation and Isotopes

journal homepage: www.elsevier.com/locate/apradiso

Survival benefit from boron neutron capture therapy for the newly diagnosed glioblastoma patients

Shinji Kawabata [a,*], Shin-Ichi Miyatake [a], Naosuke Nonoguchi [a], Ry. Hiramatsu [a], Kyoko Iida [a], Shiro Miyata [a], Kunio Yokoyama [a], Atsushi Doi [a], Yuzo Kuroda [a], Toshihiko Kuroiwa [a], Hiroyuki Michiue [b], Hiroaki Kumada [c], Mitsunori Kirihata [d], Yoshio Imahori [e], Akira Maruhashi [f], Yoshinori Sakurai [f], Minoru Suzuki [f], Shin-Ichiro Masunaga [f], Koji Ono [f]

[a] Department of Neurosurgery, Osaka Medical College, 2-7 Daigaku-machi, Takatsuki, Osaka, Japan
[b] Department of Neurosurgery, Okayama University, Okayama, Japan
[c] Research Reactor and Tandem Accelerator, Japan Atomic Energy Agency, Tohkai, Japan
[d] Department of Agriculture, Osaka Prefectural University, Sakai, Japan
[e] Cancer Intelligence Care Systems, Inc., Minati-ku, Tokyo, Japan
[f] Kyoto University Research Reactor Institute, Kumatori, Osaka, Japan

ARTICLE INFO

Keywords:
Glioblastoma
Boron neutron capture therapy
External beam X-ray irradiation
BPA
BSH

ABSTRACT

Objective: Since 2002–2007, we applied boron neutron capture therapy (BNCT) to >50 cases of malignant gliomas (MGs) with epithermal neutron irradiations. Recently, we showed the early radiographical improvement of malignant glioma patients by our modified BNCT, with simultaneous use of BPA (borono-phenylalanine) and BSH (sodium borocaptate). In this time, we focused on the survival benefit from BNCT for the newly diagnosed glioblastoma patients.

Methods: BNCT group including 21 newly histological confirmed glioblastoma patients treated with surgical removal followed by BNCT in Osaka Medical College during 2002–2006 period. Ten patients were treated with BNCT only, and in the other 11 patients, 20–30 Gy fractionated external beam X-ray irradiation therapy (XRT) was performed after BNCT. No chemotherapy was administered until tumor progression was observed.

Results: Treatments were well tolerated. Any kind of acute systemic or local severe toxicity were not demonstrated. Mean over all survival of the patients treated by BNCT was 20.7 and the median was 15.6 months with 2-years survival of 25%. Stratification by RPA criteria showed 6, 6, 8 and 1 patients, respectively, in classes III–VI. Three patients out of six in class III and one out of eight in class V are alive at the end point of this study. All the patients in classes IV and VI died. Median survival time for the BNCT group compared to the RTOG database was as follows: 20.6 months vs. 17.9 months for class III; 16.9 months vs. 11.1 months for class IV; 13.2 months vs. 8.9 months for class V.

Conclusion: The RTOG RPA prognostic criteria were helpful in establishing which class of glioma patients could potentially benefit from BNCT. BNCT showed a survival benefit in all of the RPA classes of the RTOG database not only for the good prognosis group.

1. Introduction

To create a breakthrough in the treatment for GB, we have been developing boron neutron capture therapy (BNCT) (Kawabata et al., 2003; Miyatake et al., 2005).

Numerous varieties of boron delivery agents have been developed and tested in experimental studies (Doi et al., 2008; Barth et al., 2005), but only two boron-containing drugs have been used clinically, sodium undecahydro-mercapto-*closo*-dodecaborate ($Na_2B_{12}H_{11}SH$ or sodium borocaptate [BSH]) and 4-dihydroxy-boryl-phenylalanine (or borono-phenylalanine [BPA]) (Barth et al., 2005). Each boron compound has defects as a BNCT agent. BSH dose not actively accumulate in GB, but passively accumulates by the destruction of blood brain barrier (BBB). On the other hand, BPA actively accumulates in tumors but its accumulation is significantly weak in the quiescent cell population of a tumor. Therefore, the simultaneous use of both compounds can increase the boron level in tumors while compensating for each other's faults. The effectiveness of the combined use of BSH and BPA was demonstrated in mouse tumor studies (Ono et al., 1999). Based on these findings in the experiments, we performed, for the first time ever, a new BNCT, in

* Corresponding author.
E-mail address: neu046@poh.osaka-med.ac.jp (S. Kawabata).

0969-8043/$ - see front matter © 2009 Published by Elsevier Ltd.
doi:10.1016/j.apradiso.2009.03.015